Environmental Science & Technology

Article

Cite This: Environ. Sci. Technol. 2019, 53, 8553−8562

pubs.acs.org/est

Reactive Oxygen Species Production from Secondary Organic Aerosols: The Importance of Singlet Oxygen

Alessandro Manfrin,[†] Sergey A. Nizkorodov,[‡] Kurtis T. Malecha,[‡] Gordon J. Getzinger,[†] Kristopher McNeill,[†] and Nadine Borduas-Dedekind*[,†,§]

[†]Institute for Biogeochemistry and Pollutant Dynamics, ETH Zurich, 8092 Zurich, Switzerland

[‡]Department of Chemistry, University of California, Irvine, California 92697, United States

[§]Institute for Atmospheric and Climate Science, ETH Zurich, 8092 Zurich, Switzerland

Supporting Information

ABSTRACT: Organic aerosols are subjected to atmospheric processes driven by sunlight, including the production of reactive oxygen species (ROS) capable of transforming their physicochemical properties. In this study, secondary organic aerosols (SOA) generated from aromatic precursors were found to sensitize singlet oxygen ($^1O_2$), an arguably underappreciated atmospheric ROS. Specifically, we quantified $^1O_2$, OH radical, and H_2O_2 quantum yields within photoirradiated solutions of laboratory-generated SOA from toluene, biphenyl, naphthalene, and 1,8-dimethylnaphthalene. At 5 mg_C L^{-1} of SOA extracts, the average steady-state concentrations of $^1O_2$ and of OH radicals in irradiated solutions were $3 \pm 1 \times 10^{-14}$ M and $3.6 \pm 0.9 \times 10^{-17}$ M, respectively. Furthermore, ROS quantum yields of irradiated ambient PM_{10} extracts were comparable to those from laboratory-generated SOA, suggesting a similarity in ROS production from both types of samples. Finally, by using our measured ROS concentrations, we predict that certain organic compounds found in aerosols, such as amino acids, organonitrogen compounds, and phenolic compounds have shortened lifetimes by more than a factor of 2 when $^1O_2$ is considered as an additional sink. Overall, our findings highlight the importance of SOA as a source of $^1O_2$ and its potential as a competitive ROS species in photooxidation processes.

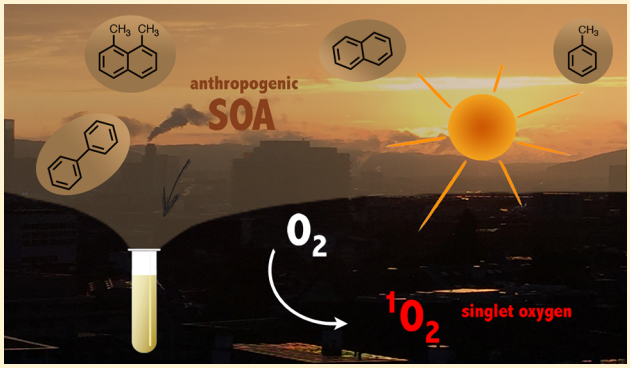

INTRODUCTION

Organic aerosols are ubiquitous in the atmosphere and represent up to 90% of the submicron particulate mass.[1] They can scatter solar radiation thereby impacting climate directly but also act as cloud condensation nuclei and impact climate indirectly. It is thus important to understand the chemical and physical properties of organic aerosols and how these properties are modified by atmospheric processing, such as solar irradiation,[2,3] heterogeneous oxidation,[4,5] hygroscopic growth,[6,7] aqueous phase processing,[8,9] etc. Chemical aging of organic aerosols can proceed by gas phase partitioning and reactive uptake of oxidants such as hydroxyl radical and ozone. Yet, there is now a recognition that chemical reactions initiated within the particle phase can dominate aging processes and consequently alter the physicochemical properties of the aerosol.[10−12]

The aqueous phase photochemistry of organic aerosols is driven by solar UV radiation and is thus limited to photons with wavelengths upward of 290 nm. Direct photolysis of organic peroxides and of H_2O_2 can generate aqueous phase OH radicals, a highly reactive and unselective oxidant. Light absorption by chromophoric organic species can yield triplet state organic matter capable of oxidizing organic material as well as producing singlet oxygen ($^1O_2$).[13−15] Up to now, atmospheric $^1O_2$ has been quantified in cloudwater,[16] fogwater,[17,18] rainwater,[19] and road dust[20] and very recently in particulate matter.[12] $^1O_2$ can also oxidize polyaromatic hydrocarbons within organic aerosols[21] to form secondary organic aerosol (SOA) from aqueous reactions of biogenic organic compounds.[22] Furthermore, $^1O_2$ is known to selectively undergo cycloaddition type reactions, which are well characterized in the context of biology.[23] This oxidant could affect the fate of aerosol tracers, pollutants within aerosols, and toxins.[17,20,22] In addition, $^1O_2$ is an important oxidant when studying the fate of pollutants in aquatic environments such as surface waters as well as when understanding oxidative stress health complications within the human body.[10,11,23−26]

Received: March 15, 2019
Revised: July 7, 2019
Accepted: July 15, 2019
Published: July 15, 2019

DOI: 10.1021/acs.est.9b01609
Environ. Sci. Technol. 2019, 53, 8553−8562

In aquatic environments, dissolved organic matter can sensitize $^1O_2$ with concentrations typically around 10^{-14} M. We hypothesized that $^1O_2$ could also be sensitized by chromophoric SOA. Indeed, we found that anthropogenic SOA produced from aromatic atmospheric precursors efficiently sensitized $^1O_2$ with quantum yields comparable to dissolved organic matter. Our goal was to quantify $^1O_2$ within irradiated SOA and particulate matter extracts and to evaluate whether $^1O_2$-mediated processes are competitive with other processes leading to the degradation of key organic aerosol tracers in SOA particles.

MATERIALS AND METHODS

SOA Preparation and Collection. The SOA samples were prepared by the photooxidation of toluene, biphenyl, naphthalene, 1,8-dimethylnaphthalene, and α-pinene inside a smog chamber at UC Irvine, using a previously described procedure.[27] The aromatic compounds were chosen based on their hypothesized ability to form sensitizing molecules, such as aromatic quinones, as well as on their atmospheric relevance from anthropogenic sources. In addition, 1,8-dimethylnaphthalene was added to the list to investigate the role of 1,4-quinone type products on $^1O_2$ production. 1,8-Dimethylnaphthalene has two additional methyl groups preventing the formation of 1,4-quinone compared to naphthalene. Furthermore, α-pinene was chosen as a control nonaromatic precursor to generate SOA.

Briefly, aromatic compound vapors and oxidant precursor H_2O_2 were mixed in a 5 m^3 Teflon FEP. The chosen starting mixing ratios (Table S1) were relatively high to produce requisite amount of material (~3 mg) for the photochemical experiments. The precursors was irradiated with UVB lamps (centered at 310 nm; FS40T12/UVB, Solar Tec Systems, Inc.) for 2 to 3 h at room temperature. Once sufficient particle mass concentration was achieved, the particles were collected on 0.2 μm pore size PTFE filters (FGLP04700 from Millipore) at 15 L/min for 3 to 4 h (Table S1). The filters were vacuum sealed and kept frozen until extraction, and the extract solutions were stored at 4 °C (section 2 in SI).

Ambient PM Sampling. PM_{10} samples were collected on quartz microfiber filters 150 mm (Whatman) with a High Volume Sampler Digitel DH 77 (Digitel Elektronik GmbH). PM_{10} (24 h) samples were taken on November 29, 2017 and on March 4, 2018 in Roveredo in the canton of Graubünden in Switzerland. Sampling dates were chosen when no extraordinary events occurred, and thus, the two selected filters can be regarded as typical particulate matter samples for this site (section 3 in SI fur further site details).

Extraction of SOA and PM_{10} Filters. Both the SOA and PM_{10} filters were extracted in glass Schott bottles with nanopure 18.2 ohm-cm milli-Q water and subsequently further diluted to exactly 5 mg_C L^{-1}. The submerged filters were then placed on a lab-shaker (Adolf Kühne AG) for about 3 h at 250 rotations per minute to obtain the water extractable components. The filters were then removed using sterilized tweezers, and the nonpurgeable organic carbon (NPOC) content in the extracts was measured using a total organic carbon (TOC) analyzer (Shimadzu, model TOC-L CSH). NPOC calibrations were done with a recrystallized solution of dipotassium phthalate, and NPOC detection limits of 1σ were <0.01 mg_C L^{-1}. Extracts were refrigerated at 4 °C until use. We tested the effect of storage on the sensitizing ability of the solution and concluded that no change in the sensitizing ability of the mixtures was observed after 1 month of storage (Table S3).

Irradiation Experiments. All extracts and reference compounds were irradiated with a SMART narrow-band hand-held lamp at 311 nm at a distance of 2 cm from a rotating sample holder. Experiments measuring $^1O_2$ steady-state concentrations were also performed with ten bulbs of 365 nm UVA broad band in a Rayonet photoreactor for comparison. The relative intensity spectra of both the 311 nm lamp and the 365 nm broadband bulbs as a function of wavelength were recorded (Figure S4). For the determination of quantum yields, we favor the use of a single wavelength lamp over a broadband source to simplify the rate of light absorption calculation, leading to fewer errors and thus more accurate quantum yield values. Furthermore, we argue that our quantum yield measurements represent upper limits due to the use of 311 nm wavelength. In fact, 311 nm is UVB irradiation, the highest energy range reaching the troposphere and the surface of the planet. Finally, the overlap between the SOA absorbance and the solar spectral flux is optimal between 310 and 340 nm (Figure S2), where the 311 nm lamp is indeed irradiating (section 4 in the SI).

Quantification of $^1O_2$ Steady-State Concentrations. Steady-state $^1O_2$ concentrations were determined for SOA extracts, solutions of SOA precursor compounds, solutions of two reference materials, specifically juglone and Suwannee River fulvic acid (SRFA), as well as extracts from two ambient PM_{10} filters. Steady-state experiments were conducted at room temperature in individual borosilicate test tubes using furfuryl alcohol (FFA, 100 μM) as a probe for $^1O_2$[28] and extracted organic material at a NPOC concentration of 5 mg_C L^{-1} as the $^1O_2$ sensitizer. The concentration of SOA samples was chosen (1) to be comparable to previously measured TOC for cloud waters,[29] (2) to give measurable $^1O_2$ production with consequent appreciable FFA degradation, and (3) to operate at the exact same NPOC concentration for all extracts. Solutions were irradiated at 311 nm, and 80 μL aliquots were sampled every 30 min and analyzed for FFA concentration using ultra high-pressure liquid chromatography (UPLC, Waters ACQUITY) coupled with a photodiode array detector (Figure S3).

To account for the reaction of FFA with OH radicals, the FFA pseudo-first-order rate constants were corrected by subtracting the contribution of OH radicals to the observed decay of FFA according to $k_{obs}^{corr} = k_{obs} - (k_{rxn}^{FFA,OH} \times [OH]_{ss})$, where $k_{rxn}^{FFA,OH} = 1.5 \times 10^{10}$ M^{-1} s^{-1},[30] and $[OH]_{ss}$ is the concentration determined as described in Quantification of OH Radical Steady-State Concentrations and Quantum Yields. Steady-state $^1O_2$ concentrations were calculated by dividing the corrected FFA pseudo-first-order rate constant (k_{obs}^{corr}) by its reaction rate constant with $^1O_2$ ($k_{rxn}^{FFA} = 1 \times 10^8$ M^{-1} s^{-1}) as in eq 1.[28]

$$[^1O_2]_{ss} = \frac{k_{obs}^{corr}}{k_{rxn}^{FFA}} \quad (1)$$

By UPLC, the detection limit of FFA was 4×10^{-7} M, calculated using 3σ of the smallest FFA calibration peak divided by the calibration slope, which corresponds to a minimum detectable $^1O_2$ steady-state concentration of 3×10^{-15} M. The kinetic solvent isotope effect was used to rule out FFA degradation by other oxidants, mainly triplet state organic matter.[30] According to Davis et al.,[31] if FFA degradation is

DOI: 10.1021/acs.est.9b01609
Environ. Sci. Technol. 2019, 53, 8553−8562

solely due to $^1O_2$ oxidation, the FFA pseudo-first-order rate constant in a solvent mixture 1:1 D_2O/H_2O (v/v) should be 1.9 times the rate observed in pure H_2O, due to the difference in $^1O_2$ lifetime in H_2O and D_2O. Therefore, we performed the FFA degradation experiments in 1:1 D_2O/H_2O (v/v) (Table S4) and found that FFA degradation is due solely to $^1O_2$ for all SOA mixtures and PM_{10} filters when irradiating at 365 nm, while there is a contribution of OH radical at 311 nm (Table S2).

6. Determination of $^1O_2$ Quantum Yield. $^1O_2$ quantum yields were determined for solutions containing SOA material, SOA precursor compounds, two reference materials, specifically juglone and Suwannee River fulvic acid, and two ambient PM_{10} filters (Table S2). Perinaphthenone (PN) was used as a reference $^1O_2$ sensitizer with a wavelength-independent quantum yield of 0.98 ± 0.08.[32] The sensitized photolysis experiments were performed in individual borosilicate test tubes using the same irradiation conditions for PN and the test mixtures. $^1O_2$ quantum yields were calculated according to eq 2

$$\phi_{^1O_2} = \frac{k_{obscorr}^{SOA}}{k_{obs}^{PN}} \times \frac{R_{abs}^{PN}}{R_{abs}^{SOA}} \times \phi_{PN} \quad (2)$$

where $k_{obscorr}^{SOA}$ and k_{obs}^{PN} are the corrected observed degradation rate constants for FFA in the presence of SOA material and PN, and R_{abs}^{SOA} and R_{abs}^{PN} are the rates of light absorption for SOA and PN (section 4.1 in SI).

7. Quantification of OH Radical Steady-State Concentrations and Quantum Yields. OH radicals were quantified using the 311 nm light source. According to the method described by Page at al.,[33] potassium terephthalate (TPA) was added to the solution and used as an OH radical probe. The reaction of OH radicals with TPA produces hydroxyterephthalate (hTPA), which was monitored over time by UPLC-PDA (Waters ACQUITY). The rate of hTPA production (R_{hTPA}) was measured for seven TPA concentrations, ranging from 20 to 400 μM (Figure S6). The OH radical production rate (R_{OH}) was determined using the asymptote of the curve generated from R_{hTPA} plotted against TPA concentration (Figure S6b). The slopes of the curves in Figure S7 were multiplied by R_{OH} and by the reaction rate constant of TPA with OH radicals to obtain the OH radical scavenging rate constant of the SOA extracts, k'_{OH}. $[OH]_{ss}$ under conditions of no probe were obtained by dividing R_{OH} by k'_{OH}. The hydroxyl radical steady-state concentrations, $[OH]_{ss}$, was also determined under conditions of no probe, following the approach described by Zhou and Mopper (section 4.2.1. in SI).[34] Under our experimental conditions, the limit of detection of hTPA is 1×10^{-8} M, which corresponds to a minimum detectable OH radical steady-state concentration of 3×10^{-18} M.

The OH radical generation quantum yields were determined for all the extracts according to eq 3

$$\phi_{OH} = R_{OH}/R_{abs} \quad (3)$$

where R_{OH} is the rate of OH radical production and R_{abs} is the rate of light absorption of the solution (section 4.2 in SI).

8. Quantification of Hydrogen Peroxide Production and Quantum Yield. Hydrogen peroxide production was quantified using the horseradish peroxidase (HRP)-Amplex Red method.[35,36] A horseradish peroxidase solution was prepared by combining 10 μL of a 10 mM Amplex Red solution in DMSO, 20 μL of 10 U/mL horseradish peroxidase solution in 50 mM phosphate buffer pH 7.4, and 1 mL of 50 mM phosphate buffer at pH 7.4. Each sample was irradiated at 311 nm, and 50 μL aliquots were taken every 30 min. Then, 50 μL of the horseradish peroxidase mixture was added to the aliquot. In the presence of the horseradish peroxidase enzyme, Amplex Red reacts with H_2O_2 to produce fluorescent resorufin with a yield of ~100%.[36] After incubation in darkness for at least 30 min to produce resorufin, the samples were analyzed for resorufin using ultra high-pressure liquid chromatography (UPLC, Waters ACQUITY) coupled with a photodiode array detector (Figure S8). The detection limit of H_2O_2 was 2×10^{-7} M under our experimental conditions.

Hydrogen peroxide quantum yields were obtained as the ratio of the hydrogen peroxide production rate, measured with the HRP-Amplex Red method, and the rate of light absorption using eq 4 (Table S6 and section 4.3 in SI).

$$\phi_{H_2O_2} = R_{H_2O_2}/R_{abs} \quad (4)$$

RESULTS AND DISCUSSION

$^1O_2$ Production from SOA Extracts. The filter extracts from toluene, biphenyl, naphthalene, and 1,8-dimethylnaphthalene SOA efficiently sensitized $^1O_2$ and produced OH radicals as well as peroxides upon irradiation with single wavelength UVB light at 311 nm. The $^1O_2$ steady-state concentrations, measured in these conditions for 5 mg_C L^{-1} solutions of SOA extracts, ranged between 1.1×10^{-14} and 4.5×10^{-14} M with an average of $(3 \pm 1) \times 10^{-14}$ M (Figure 1).

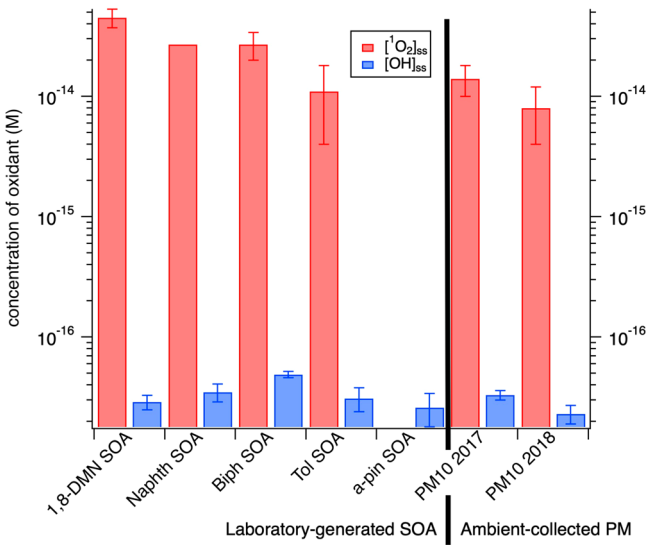

Figure 1. Steady-state concentrations of $^1O_2$ and OH radicals quantified for irradiation at 311 nm within laboratory-generated SOA and ambient-collected PM_{10} filters. No quantifiable FFA degradation was observed with α-pinene SOA.

All SOA extracts from aromatic precursors showed $^1O_2$ quantum yields ranging between 1.2×10^{-2} and 3.2×10^{-2} (Table 1, Figure 2). These results show that laboratory-generated anthropogenic SOA material can generate a significant amount of $^1O_2$ when irradiated with UV light, an observation currently underappreciated in aerosol ROS chemistry.

DOI: 10.1021/acs.est.9b01609
Environ. Sci. Technol. 2019, 53, 8553−8562

Table 1. Summary of Measured ROS Steady-State Concentrations and Quantum Yields for SOA samples and PM_{10} Filters[a]

Entry	TOC (mg_C/L)	$[^1O_2]_{ss}$ (10^{-14} M)	Φ $^1O_2$ (10^{-2})	$[OH\cdot]_{ss}$ (10^{-17} M)	Φ OH· (10^{-5})	Φ H_2O_2 (10^{-4})
1,8-DMN SOA	5	4.5 ± 0.8	3 ± 1	2.9 ± 0.4	4.6 ± 0.9	4.5 ± 0.4
1,8-DMN	5	2.2 ± 0.6	0.3 ± 0.2	<0.3	nd	1.5 ± 0.6
Naphthalene SOA	5	2.7	2.3	3.5 ± 0.6	6.3 ± 1.0	3.5 ± 0.3
Biphenyl SOA	5	2.7 ± 0.7	2.3 ± 0.7	4.9 ± 0.3	5.1 ± 1.0	2.5 ± 0.2
Toluene SOA	5	1.1 ± 0.7	1.2 ± 0.3	3.1 ± 0.7	6.8 ± 1.3	2.6 ± 0.3
α-Pinene SOA	5	<0.3	nd	2.6 ± 0.8	nd	4.3 ± 0.4
PM_{10} filter Nov 2017	5	1.4 ± 0.4	4.5 ± 0.4	3.3 ± 0.3	11 ± 4	3.9 ± 0.6
PM_{10} filter Mar 2018	5	0.8 ± 0.4	4.0 ± 0.3	2.3 ± 0.4	24 ± 5	6.5 ± 0.7

[a]The error reported for $[^1O_2]_{ss}$ represents the standard deviation of 3 measurements, while the errors reported for quantum yields are propagated errors. No uncertainty is associated with naphthalene SOA because not enough material was collected to repeat at least three measurements; nd = not determined.

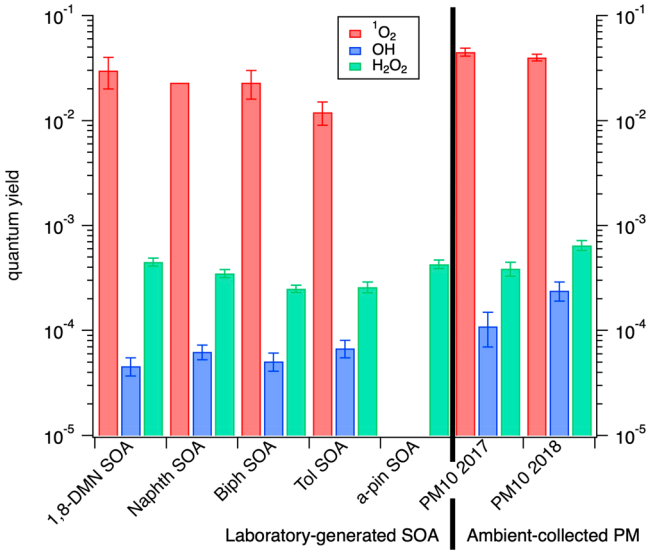

Figure 2. Quantum yields of each oxidant measured at 311 nm for laboratory-generated SOA and ambient-collected PM_{10}.

For comparison, the $^1O_2$ quantum yield of Suwannee River fulvic acid (SRFA), a commercially available and well-studied dissolved organic matter within the field of aquatic photochemistry, was 3.4×10^{-2} under identical experimental conditions (Table S2), consistent with the literature range of 1.0×10^{-2} to 4.0×10^{-2}.[37−41] We can conclude that the $^1O_2$ quantum yield measured for SOA generated from aromatic precursors compares well with $^1O_2$ quantum yields known for chromophoric dissolved organic matter.

In addition, α-pinene SOA was used as a control nonaromatic precursor-generated SOA (Table 1, Table S2). We did not expect α-pinene SOA to sensitize $^1O_2$, since compounds found in this SOA do not contain conjugated double bonds or aromatic systems and indeed have limited ability to absorb light, as shown by its UV−vis spectra (Figures S1 and S2) and the specific ultraviolet absorbance at 254 nm ($SUVA_{254}$) (Table S8). As expected, no quantifiable $^1O_2$ production could be observed when α-pinene SOA was used as a $^1O_2$ sensitizer.

Furthermore, we conducted $^1O_2$ experiments with the pure precursor compounds of the SOA filters (toluene, biphenyl, naphthalene, and 1,8-dimethylnaphthalene) in aqueous solutions at a concentration of 5 $mg_C\ L^{-1}$. These compounds did not show any $^1O_2$ production, except for 1,8-dimethylnaphthalene which displayed $^1O_2$ sensitizing ability, although much lower than its corresponding SOA material. Specifically, a solution of 1,8-dimethylnaphthalene showed a $^1O_2$ quantum yield of 0.3×10^{-2}, 1 order of magnitude smaller than the SOA material prepared by oxidation of 1,8-dimethylnaphthalene (3.2×10^{-2}). This result suggests that photosensitizing moieties are produced during the photooxidation of the SOA precursor compounds inside the smog chamber, which is known for toluene oxidation products.[42,43]

OH Radicals and H_2O_2 Production from SOA Extracts. In the context of evaluating the relevance of $^1O_2$ within ROS produced in irradiated SOA and PM_{10} extracts, we also quantified the production of OH radicals and H_2O_2. All irradiated SOA samples at 311 nm produced steady-state concentrations of hydroxyl radicals between 2.6×10^{-17} to 4.9×10^{-17} M (Figure 1). Note that these concentrations are 3 orders of magnitude lower than the steady-state concentrations of $^1O_2$, quantified for the same aqueous SOA samples. OH radical quantum yields were also calculated and ranged between 4.6×10^{-5} and 6.8×10^{-5}, 3 orders of magnitude smaller than $^1O_2$ (Figure 2).

In addition, biphenyl and 1,8-dimethylnaphthalene SOA extracts were found to have slightly lower quantum yields for producing OH radicals (5.1×10^{-5} and 4.6×10^{-5}, respectively), compared to naphthalene and toluene SOA (6.3×10^{-5} and 6.8×10^{-5}, respectively) (Table 1 and Figure 2). Irradiation of solutions of pure organic compounds that served as SOA precursors (toluene, biphenyl, naphthalene, and 1,8-dimethylnaphthalene) did not show any OH radical production under the same experimental conditions. This result further supports the fact that the ability of producing ROS is derived from functional groups formed in the aerosol production process.

The competition kinetic approach used to determine $[OH]_{ss}$ and OH radical production rates allowed us to estimate the OH radical scavenging rate constant of SOA mixtures (k'_{OH}). Values obtained ranged between 3.5 and $8.9 \times 10^5\ s^{-1}$ (Table S5), similar to dissolved organic matter samples and fog waters by Arakaki et al.[44] We further calculated the ratio between k'_{OH} and the NPOC, finding values between 3.0 and 7.5×10^8 L $M_C^{-1}\ s^{-1}$ (Table S5), in agreement with previously reported values for dissolved organic matter,[44] fog waters,[44] and particle extracts.[12]

Furthermore, all anthropogenic and biogenic SOA samples were able to generate H_2O_2, although to different extents. Since H_2O_2 concentrations increased with irradiation time, no steady-state concentrations can be determined (Figure S8). Naphthalene, 1,8-dimethylnaphthalene, and α-pinene SOA had similar H_2O_2 quantum yields, while biphenyl and toluene SOA showed a lower activity (Table 1 and Figure 2). As expected,

DOI: 10.1021/acs.est.9b01609
Environ. Sci. Technol. 2019, 53, 8553−8562

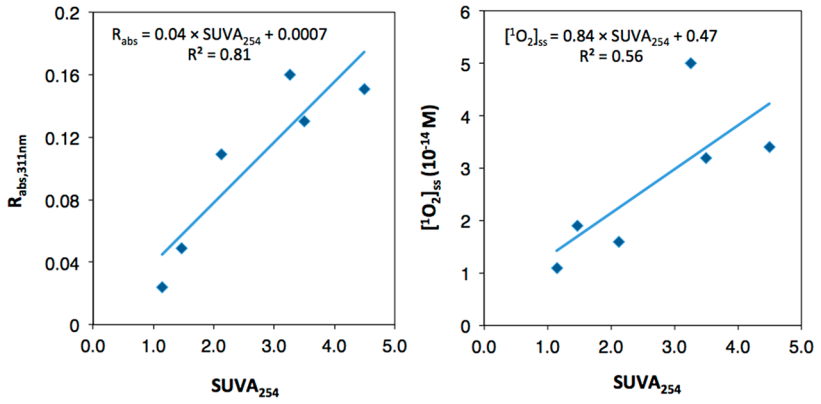

Figure 3. Left: Correlation plot of the rate of light absorbance at 311 nm of SOA and PM_{10} extracts (total of six extracts) as a function of SUVA at 254 nm. Right: Correlation plot of $^1O_2$ steady-state concentrations of the same six extracts as a function of $SUVA_{254}$.

the pure compounds did not produce H_2O_2, except for 1,8-dimethylnaphthalene with a quantum yield of 1.5×10^{-4}. The H_2O_2 quantum yields are 1 order of magnitude larger than the OH radical quantum yields and ranged between 2.5×10^{-4} and 4.5×10^{-4}.

When comparing OH and $^1O_2$ quantum yields and steady-state concentrations, we observed that the OH radical quantum yields and resulting concentrations were 3 orders of magnitude smaller (Table 1, Figure 2). The higher concentration of $^1O_2$ is counter balanced by its higher substrate selectivity and lower reactivity,[45] which make OH radicals and $^1O_2$ competitive oxidants for processing air pollutants and tracers.

In addition, a fraction of the OH radicals are likely generated by H_2O_2 photolysis. If this photolysis is the rate limiting step, which is a reasonable assumption based on H_2O_2 concentrations increasing with time, then one could expect higher quantum yields for H_2O_2 compared to OH radicals.

$^1O_2$, OH Radical, and H_2O_2 Comparison between SOA and PM_{10} Extracts. Our results suggest the importance of $^1O_2$ as an oxidant in anthropogenic SOA. Because these aerosols were generated within a smog chamber at high concentrations and may not accurately represent the real atmosphere, we extended our study to two 24 h-integrated PM_{10} filters, collected in Graubünden, Switzerland. Irradiated PM_{10} filter extracts at 311 nm produced ROS (Table 1, Figure 2). We found that steady-state concentrations of $^1O_2$ were comparable to those for SOA prepared from toluene but lower than for SOA prepared from larger aromatic compounds (Figure 1). The PM_{10} extracts showed systematically higher $^1O_2$ quantum yields than SOA mixtures (Figure 2). Their average $^1O_2$ steady-state concentration and production quantum yield were 1.1×10^{-14} M and 0.043, respectively. The sensitizing ability of PM_{10} extracts further supports the importance of $^1O_2$ in atmospheric processing of organic aerosols.

The PM_{10} samples were also tested for the production of OH radicals and H_2O_2. OH radical quantum yields were on the same order of magnitude than those for the SOA mixtures, albeit two to three times higher (Table 1, Figure 2). PM_{10} samples also produced H_2O_2, with quantum yields in the range of 3.9 to 6.5×10^{-4}. These findings indicate that ROS quantum yields measured from the laboratory-generated SOAs are comparable to quantum yields from actual field-collected atmospheric particulate matter.

Origin of SOA and PM_{10} Extracts' Sensitizing Ability. In order to understand the origin of the sensitizing ability of SOA, we evaluated the aromaticity of SOA samples, since it is known that aromatic structures are important light-absorbing moieties and promote the photosensitizing ability of organic compounds.[46] The photooxidation of aromatic hydrocarbons can produce compounds with a retained aromatic moiety and compounds with ring-opened and oxidized functionalities. For example, products of oxidation of naphthalene include substituted naphthalene compounds, such as naphthols, as well as substituted benzene compounds, such as hydroxy benzoic acids.[47] The gas phase mechanism of toluene oxidation also can similarly lead to phenolic type compounds.[48] In this section, we discuss the specific ultraviolet absorbance at 254 nm ($SUVA_{254}$), the aromaticity equivalent (X_c), and the sensitizing ability of juglone to assess the origin of $^1O_2$ within chromophoric SOA and PM_{10} extracts.[49]

$SUVA_{254}$. The effective aromaticity of toluene, biphenyl, naphthalene, 1,8-dimethylnaphthalene, and α-pinene SOA samples, as well as PM_{10} filters, was estimated by calculating $SUVA_{254}$, previously used as a proxy for organic matter aromaticity.[50] The $SUVA_{254}$ was calculated by normalizing the absorbance at 254 nm with the total organic carbon of the mixture, and ranged between 1.0 and 4.5 L mg_C^{-1} m^{-1}, showing appreciable aromatic content in aromatic SOA extracts and PM_{10} filters (Table S8). The highest $SUVA_{254}$ value was found for biphenyl SOA, likely due to the presence of two independent aromatic structures capable of preserving aromaticity during photooxidation.[51] α-Pinene SOA had a low $SUVA_{254}$ value of 0.3, consistent with the absence of aromatic structures in the mixture (Table S8).

PM_{10} filters had reduced $SUVA_{254}$ values compare to SOA materials, agreeing with their lower $^1O_2$ steady-state concentrations and thus with their higher quantum yields. The same effect was previously noted in fractionated dissolved organic matter, where less aromatic fractions showed higher quantum yields due to their limited rate of light absorption.[41,52] In addition, we found a correlation between the rate of light absorption at 311 nm and the $^1O_2$ steady-state concentrations with $SUVA_{254}$ values, suggesting that an increase in aromatic content produces higher rates of light absorption and therefore higher $^1O_2$ steady-state concentrations (Figure 3). $SUVA_{254}$ values were also calculated after 4 h of irradiation at 311 and 365 nm, showing no significant change in the absorption of the mixtures (Figure S9, Table S8).

DOI: 10.1021/acs.est.9b01609
Environ. Sci. Technol. 2019, 53, 8553−8562

Table 2. Summary of Singlet Oxygen and Hydroxyl Radical Steady-State Concentrations and Quantum Yields for Atmospherically Relevant Aqueous Solutions[g]

Material	$[^1O_2]_{ss}$ (10^{-14} M)	ϕ $^1O_2$ (10^{-2})	$[OH\cdot]_{ss}$ (10^{-17} M)	ϕ OH· (10^{-5})	Reference
Cloud water	2.7−110[a]	4.8−20			Faust et al., *J. Geophys. Res.* 1992
Fog water	11−61[b]		17−77[b]	1−64	Anastasio and McGregor, *Atmos. Environ.* 2001
Rain water	≤0.27[c]		87−150[c]		Albinet and Vione, *Sci. Total Environ.* 2010
Fog water	1.1−30[b]	1.1−12	26−110[b]	15−87	Kaur et al., *Atmos. Environ.* 2017
Road dust extracts	0.83−10[d]				Cote et al., *Environ. Sci. Technol. Lett.* 2018
PM_{10} extracts	6.4−220[e]	2.2−5.7	17−79[e]	6.2−35	Kaur et al., *Atmos. Chem. Phys.* 2019
SOA extracts	1.1−4.5[f]	1.2−3	2.6−4.9[f]	4.6−6.8	This work
PM_{10} extracts	0.8−1.4[f]	4.0−4.5	2.2−3.3[f]	11−24	This work

[a]Midday, equinox-normalized steady-state concentration. [b]Winter solstice-normalized steady-state concentration. [c]Values obtained with UV-A lamps at 365 nm with a photon flux of 1.6×10^{-5} E L^{-1} s^{-1} [d]Steady-state concentration obtained by irradiation with a solar simulator [e]Steady-state concentration measured in D_2O irradiating with a xenon arc lamp [f]Steady-state concentration obtained by irradiation at 311 nm [g]The values are reported as ranges; note that steady-state concentrations are dependent on the TOC of the sample and the illumination method.

Aromaticity Equivalent. High resolution mass spectrometry (HRMS) analysis (section 6 of SI) of the SOA samples was performed and yielded mass spectra of a complex mixture of oxidized organic compounds, with masses up to 300 Da (Figure S10). We calculated the aromaticity equivalent values (X_c) from assigned molecular formulas (Figure S11).[49] For aromatic SOA materials, X_c values were ≥2.5, representative of the threshold for the presence of aromatics and condensed aromatics in the mixture.[49] The X_c values were calculated at 0 and at 4 h of irradiation for toluene, biphenyl, naphthalene, and 1,8-dimethylnaphthalene SOA extracts. As for the $SUVA_{254}$ values, we observed no significant changes in X_c values after 4 h of irradiation (Figure S11), indicating no depletion in the aromatic content of the mixtures. This evidence is in good agreement with the constant rate of FFA degradation over time, implying a steady-state concentration of $^1O_2$ when SOA samples are irradiated over the time scale of 4 h. Since the $^1O_2$ sensitizing ability of SOA is not measurably depleted during irradiation, the ROS produced did not modify the sensitizing properties within our experimental time scales. We also plotted for the four SOA extracts the H/C vs O/C ratios (Figure S12), the nominal carbon oxidation state vs carbon number (Figure S13), and aromaticity index vs carbon number (Figure S14), all with the same conclusion.

Juglone as a Sensitizer. We identified a peak at m/z of 174.0321 in naphthalene SOA, which we tentatively assigned to juglone, a hydroxy-benzoquinone known as a naphthalene oxidation intermediate.[53] We tested the ability of juglone to produce $^1O_2$ and measured a $^1O_2$ steady-state concentration of $7.3 \pm 0.9 \times 10^{-14}$ M and a quantum yield of $11 \pm 2 \times 10^{-2}$ (Table S2). The $^1O_2$ steady-state concentration of juglone fell in the range of the measured SOA extracts. The quantum yield of juglone was higher than the quantum yield of the SOA extracts since as a pure compound, it did not absorb as much light as organic matter without sensitizing $^1O_2$. This observation is consistent with our hypothesis that the presence of aromatics is important for sensitizing $^1O_2$. Yet, if 1,4-quinone moieties were the major sensitizing moiety, a difference between the $^1O_2$ concentrations of naphthalene and 1,8-dimethylnaphthalene would have been observed, since 1,8-dimethylnaphthalene cannot form 1,4 quinones. Since this difference was not observed, we can only state that aromatic quinones, such as juglone, are likely one of many classes of $^1O_2$ sensitizers in SOA derived from aromatic precursors.

Comparison of $^1O_2$ and OH Radical Quantum Yields with the Literature. To place our findings in the context of different aerosol types and understand the importance of SOA-produced ROS in the oxidation of air pollutants and particulate matter, we compare our ROS steady-state concentrations and quantum yields with previously published measurements of fog, rain, and cloud waters as well as road dust (Table 2). Faust and Allen reported the first measurement of $^1O_2$ steady-state concentration in cloudwater,[16] with values comparable to this work for SOA and PM_{10} extracts. However, the reported quantum yields span a wider range, likely due to the variability of the sampling locations. Anastasio and McGregor measured $^1O_2$ and OH radical steady-state concentrations in fog waters,[18] using the same FFA method employed in this study, and reported 4 to 20 times higher concentrations but comparable OH radical quantum yields. Albinet and Vione measured $^1O_2$ and OH radical steady-state concentrations in rainwater and detected no $^1O_2$ but a high concentration of OH radicals.[19] Kaur and Anastasio measured the same oxidants in fogwater samples collected in Davis, California,[17] finding an average $^1O_2$ quantum yield of 4.2×10^{-2}, which compares well with our SOA and PM_{10} extracts. In addition, the OH radical quantum yields reported for fog waters were six times larger than those for our SOA extracts. This difference could potentially be ascribed to the presence of fewer OH radical sources in SOA than in fogwater. Kaur and Anastasio indeed reported that 70% of the OH radical production was due to NO_2^- and NO_3^- in fog waters, while these anions are not present in our SOA extracts. Furthermore, Cote et al. reported the $^1O_2$ production from aqueous road dust and showed that irradiated extracts generated $^1O_2$ with steady-state concentrations of 1×10^{-13} M;[20] however, $^1O_2$ quantum yields were not reported and therefore experimental conditions cannot be directly compared at this time. Most recently, Kaur et al. quantified $^1O_2$, OH radicals and triplet state organic matter within fog and particulate matter in Davis, California.[12] They obtained higher $^1O_2$ steady-state concentrations, in agreement with their use of 50% D_2O as a solvent, which extends $^1O_2$ lifetime by a factor of 2, and their use of a xenon lamp.

Atmospheric Implications. In this work, we tested and verified the hypothesis that SOA generated from aromatic compounds are capable of photosensitizing $^1O_2$. The measured concentrations of $^1O_2$ were 3 orders of magnitude higher than those of OH radical, indicating that $^1O_2$ could play a role in oxidizing air pollutants and tracers. To compare the relevance of these two oxidants for the fate of environmentally relevant pollutants and air tracers, we performed a kinetic box model for organic compounds with known $^1O_2$ and OH radical

DOI: 10.1021/acs.est.9b01609
Environ. Sci. Technol. 2019, 53, 8553−8562

reaction rate constants (Figure 4, Table S9). The goal is to highlight the potential of $^1O_2$ as a relatively important oxidant

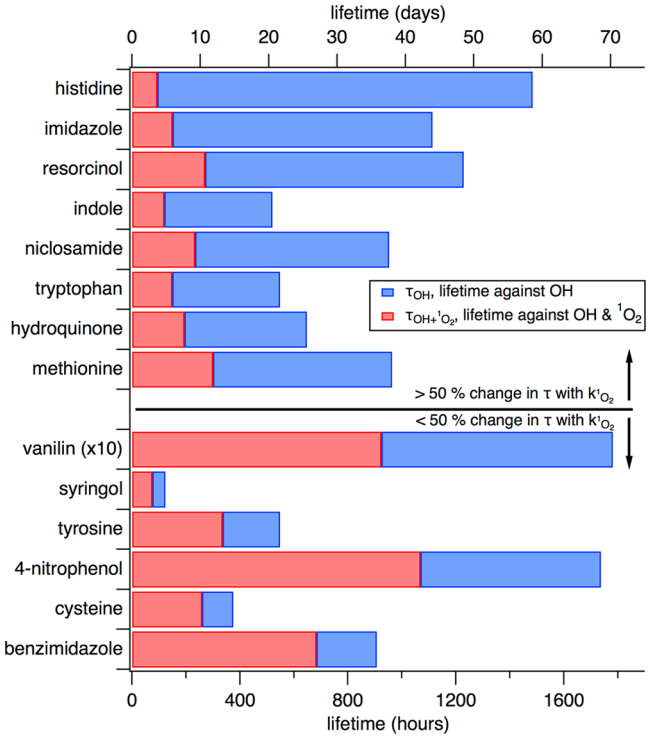

Figure 4. Results of a kinetic box model for $^1O_2$ and OH radical contribution to the environmental lifetimes of selected tracers. The 14 compounds were selected because they have known OH radical and $^1O_2$ reaction rate constants in water. In addition, the compounds were categorized into two categories depending on whether their overall lifetime was affected by more or by less than 50% with the consideration of $^1O_2$ as sink.

in organic aerosol processing. For $^1O_2$ and OH radical steady-state concentrations, we used the average values from our SOA measurements of 3×10^{-14} M and 4×10^{-17} M, respectively, and we used literature reaction rate constants for the following organic compounds: benzimidazole, 4-nitrophenol, vanillin, imidazole, indole, syringol, histidine, resorcinol, niclosamide, tryptophan, hydroquinone, methionine, tyrosine, and cysteine.[54−70] Some of these compounds are potentially found in atmospheric aerosols, such as benzimidazole, cysteine,[71] nitrophenols,[72,73] tyrosine,[71] syringol, and vanillin.[74,75] We opted not to consider H_2O_2 as part of this box model because of its low concentrations and low reactivity with organics compared to the other two ROS.

The 14 compounds studied here could be classified into two categories: overall lifetimes against ROS reduced by (1) more than 50% and by (2) less than 50%, when including $^1O_2$ as a sink (Figure 4). In general, the lifetimes of compounds which contain electron-rich aromatic rings such as histidine, imidazole, resorcinol, indole, tryptophan, and hydroquinone are strongly affected by the presence of $^1O_2$ (Figure 4). Of note, histidine's lifetime against OH is 59 days, whereas its lifetime against OH radicals and $^1O_2$ is 4 days, indicating that $^1O_2$ is the major sink for histidine in proteinaceous aqueous aerosols. Furthermore, other amino acids (e.g., tryptophan, methionine), organo-nitrogen compounds (imidazole, indole, niclosamide), and phenolic compounds (hydroquinone, resorcinol) have shortened lifetimes by more than a factor of 2 when $^1O_2$ reactivity is considered in their overall fate (Figure 4). The second category of compounds with lifetimes affected to a lesser extent by $^1O_2$ reactivity also include amino acids and phenolic compounds, and thus the prediction of the effect of an additional sink against $^1O_2$ on a single compound basis remains difficult.

To further corroborate the importance of $^1O_2$ as a potential atmospheric oxidant for organic aerosol processing, Kaur et al. recently came to the same conclusion when looking at the contributions of OH radicals, $^1O_2$, and triplet state organic carbon to PM and fogwater processing.[12] Therefore, the omission of $^1O_2$ reactivity in SOA processing models could lead to the overestimation of the lifetimes of aromatic pollutants and atmospheric aerosol tracers. We also recommend that $^1O_2$ rate coefficients with key atmospheric pollutants be the focus of further organic aerosol kinetics research. It is also likely that $^1O_2$ is participating in atmospheric aging of organic aerosols.[76]

From the results reported in this work, it is clear that irradiated aromatic SOA can produce ROS, including $^1O_2$, in the atmosphere. In the literature, photochemical processing of organic aerosols has been primarily attributed to OH radicals from organic peroxide decomposition and Fenton chemistry,[77] but it is likely that $^1O_2$ is also participating in the same photochemical processing and playing an important role in the oxidation of certain air pollutants. $^1O_2$ is a selective oxidant and typically shows reaction rate constants with organic molecules 2 to 3 orders of magnitude smaller than those of the OH radical; however, the measured $^1O_2$ steady-state concentrations here and in other recent publications are about 3 orders of magnitude larger than those of the OH radical (see Table 2). Consequently, we expect $^1O_2$ to be a competitive oxidant to OH radicals.

■ ASSOCIATED CONTENT

Supporting Information

The Supporting Information is available free of charge on the ACS Publications website at DOI: 10.1021/acs.est.9b01609.

UV−vis spectra of SOA samples, quantum yields calculations for SOA, SRFA, juglone, PM_{10} filters and precursor compounds, rate constants used in the model box calculation, $SUVA_{254}$, MS data (PDF)

■ AUTHOR INFORMATION

Corresponding Author

*E-mail: nadine.borduas@usys.ethz.ch. Phone: +41 44 632 7315. Twitter: @nadineborduas.

ORCID

Alessandro Manfrin: 0000-0003-1084-4787
Sergey A. Nizkorodov: 0000-0003-0891-0052
Gordon J. Getzinger: 0000-0002-5628-1425
Kristopher McNeill: 0000-0002-2981-2227
Nadine Borduas-Dedekind: 0000-0001-9302-368X

Author Contributions

The manuscript was written through contributions of all authors. All authors have given approval to the final version of the manuscript.

Funding

We acknowledge the Swiss National Science Foundation (Grant no. 200020_159809) and SNSF Ambizione Grant

DOI: 10.1021/acs.est.9b01609
Environ. Sci. Technol. 2019, 53, 8553−8562

(PZ00P2_179703) as well as the American National Science Foundation (NSF) through the Graduate Research Fellowship Program and NSF grant AGS-1853639.

Notes

The authors declare no competing financial interest.

■ ACKNOWLEDGMENTS

The authors would like to thank Jeroen van den Wildenberg for his technical help and Rachele Ossola for helpful discussions. We acknowledge the assistance of Dr. Ulrich Krieger with the collection of the PM_{10} filters. We also acknowledge Dr. Kyle Moor for wavelength dependence quantum yield discussions and Prof. Christy Remucal for mass spectrometry discussions. We further thank the anonymous reviewers for insightful suggestions.

■ ABBREVIATIONS

FFA	furfuryl alcohol
SOA	secondary organic aerosol
TOC	total organic carbon
NPOC	nonpurgeable organic carbon
ROS	reactive oxygen species
SRFA	Suwannee River fulvic acid
PM_{10}	particulate matter smaller than 10 micrometers in diameter
TPA	potassium terephthalate
hTPA	hydroxyterephthalate
$SUVA_{254}$	specific ultraviolet absorbance at 254 nm
UPLC	ultra high-pressure liquid chromatography
PDA	photodiode array

■ REFERENCES

(1) Jimenez, J. L.; Canagaratna, M. R.; Donahue, N. M.; Prevot, A. S. H.; Zhang, Q.; Kroll, J. H.; DeCarlo, P. F.; Allan, J. D.; Coe, H.; Ng, N. L. Evolution of Organic Aerosols in the Atmosphere. *Science* **2009**, *326* (5959), 1525−1529.

(2) George, C.; D'Anna, B.; Herrmann, H.; Weller, C.; Vaida, V.; Donaldson, D. J.; Bartels-Rausch, T.; Ammann, M. Emerging Areas in Atmospheric Photochemistry. In *Atmospheric and Aerosol Chemistry*; McNeill, V. F., Ariya, P. A., Eds.; Topics in Current Chemistry; Springer: Berlin Heidelberg, 2012; pp 1−53.

(3) Jokinen, T.; Kontkanen, J.; Lehtipalo, K.; Manninen, H. E.; Aalto, J.; Porcar-Castell, A.; Garmash, O.; Nieminen, T.; Ehn, M.; Kangasluoma, J. Solar Eclipse Demonstrating the Importance of Photochemistry in New Particle Formation. *Sci. Rep.* **2017**, *7*, 45707.

(4) George, C.; Ammann, M.; D'Anna, B.; Donaldson, D. J.; Nizkorodov, S. A. Heterogeneous Photochemistry in the Atmosphere. *Chem. Rev.* **2015**, *115* (10), 4218−4258.

(5) George, I. J.; Slowik, J.; Abbatt, J. P. D. Chemical Aging of Ambient Organic Aerosol from Heterogeneous Reaction with Hydroxyl Radicals. *Geophys. Res. Lett.* **2008**, *35* (13), 4218−4258.

(6) Cruz, C. N.; Pandis, S. N. Deliquescence and Hygroscopic Growth of Mixed Inorganic−Organic Atmospheric Aerosol. *Environ. Sci. Technol.* **2000**, *34* (20), 4313−4319.

(7) Freney, E. J.; Adachi, K.; Buseck, P. R. Internally Mixed Atmospheric Aerosol Particles: Hygroscopic Growth and Light Scattering. *J. Geophys. Res.* **2010**, *115*, D19210.

(8) Laskin, A.; Laskin, J.; Nizkorodov, S. A. Chemistry of Atmospheric Brown Carbon. *Chem. Rev.* **2015**, *115* (10), 4335−4382.

(9) Ervens, B. Modeling the Processing of Aerosol and Trace Gases in Clouds and Fogs. *Chem. Rev.* **2015**, *115* (10), 4157−4198.

(10) Herrmann, H. Kinetics of Aqueous Phase Reactions Relevant for Atmospheric Chemistry. *Chem. Rev.* **2003**, *103* (12), 4691−4716.

(11) Herrmann, H.; Schaefer, T.; Tilgner, A.; Styler, S. A.; Weller, C.; Teich, M.; Otto, T. Tropospheric Aqueous-Phase Chemistry: Kinetics, Mechanisms, and Its Coupling to a Changing Gas Phase. *Chem. Rev.* **2015**, *115* (10), 4259−4334.

(12) Kaur, R.; Labins, J. R.; Helbock, S. S.; Jiang, W.; Bein, K. J.; Zhang, Q.; Anastasio, C. Photooxidants from Brown Carbon and Other Chromophores in Illuminated Particle Extracts. *Atmos. Chem. Phys.* **2019**, *19* (9), 6579−6594.

(13) McNeill, K.; Canonica, S. Triplet State Dissolved Organic Matter in Aquatic Photochemistry: Reaction Mechanisms, Substrate Scope, and Photophysical Properties. *Environ. Sci. Process. Impacts* **2016**, *18* (11), 1381−1399.

(14) Kaur, R.; Anastasio, C. First Measurements of Organic Triplet Excited States in Atmospheric Waters. *Environ. Sci. Technol.* **2018**, *52* (9), 5218−5226.

(15) Kaur, R.; Hudson, B. M.; Draper, J.; Tantillo, D. J.; Anastasio, C. Aqueous Reactions of Organic Triplet Excited States with Atmospheric Alkenes. *Atmos. Chem. Phys.* **2019**, *19* (7), 5021−5032.

(16) Faust, B. C.; Allen, J. M. Aqueous-Phase Photochemical Sources of Peroxyl Radicals and Singlet Molecular Oxygen in Clouds and Fog. *J. Geophys. Res.* **1992**, *97* (D12), 12913−12926.

(17) Kaur, R.; Anastasio, C. Light Absorption and the Photoformation of Hydroxyl Radical and Singlet Oxygen in Fog Waters. *Atmos. Environ.* **2017**, *164*, 387−397.

(18) Anastasio, C.; McGregor, K. G. Chemistry of Fog Waters in California's Central Valley: 1. In Situ Photoformation of Hydroxyl Radical and Singlet Molecular Oxygen. *Atmos. Environ.* **2001**, *35* (6), 1079−1089.

(19) Albinet, A.; Minero, C.; Vione, D. Photochemical Generation of Reactive Species upon Irradiation of Rainwater: Negligible Photoactivity of Dissolved Organic Matter. *Sci. Total Environ.* **2010**, *408* (16), 3367−3373.

(20) Cote, C. D.; Schneider, S. R.; Lyu, M.; Gao, S.; Gan, L.; Holod, A. J.; Chou, T. H. H.; Styler, S. A. Photochemical Production of Singlet Oxygen by Urban Road Dust. *Environ. Sci. Technol. Lett.* **2018**, *5* (2), 92−97.

(21) Chen, J.; Valsaraj, K. T. Uptake and UV-Photooxidation of Gas-Phase Polyaromatic Hydrocarbons on the Surface of Atmospheric Water Films. 2. Effects of Dissolved Surfactants on Naphthalene Photooxidation. *J. Phys. Chem. A* **2007**, *111* (20), 4289−4296.

(22) Richards-Henderson, N.; Pham, A. T.; Kirk, B. B.; Anastasio, C. Secondary Organic Aerosol from Aqueous Reactions of Green Leaf Volatiles with Organic Triplet Excited States and Singlet Molecular Oxygen. *Environ. Sci. Technol.* **2015**, *49* (1), 268−276.

(23) Di Mascio, P.; Martinez, G. R.; Miyamoto, S.; Ronsein, G. E.; Medeiros, M. H. G.; Cadet, J. Singlet Molecular Oxygen Reactions with Nucleic Acids, Lipids, and Proteins. *Chem. Rev.* **2019**, *119* (3), 2043−2086.

(24) Moan, J.; Berg, K. Photochemotherapy of Cancer: Experimental Research. *Photochem. Photobiol.* **1992**, *55* (6), 931−948.

(25) Yamazaki, S.; Ozawa, N.; Hiratsuka, A.; Watabe, T. Photogeneration of 3β-Hydroxy-5α-Cholest-6-Ene-5-Hydroperoxide in Rat Skin: Evidence for Occurrence of Singlet Oxygen in Vivo. *Free Radical Biol. Med.* **1999**, *27* (3), 301−308.

(26) Devasagayam, T. P. A.; Kamat, J. P. Biological Significance of Singlet Oxygen. *Indian J. Exp. Biol.* **2002**, *40* (6), 680−692.

(27) Malecha, K. T.; Nizkorodov, S. A. Photodegradation of Secondary Organic Aerosol Particles as a Source of Small, Oxygenated Volatile Organic Compounds. *Environ. Sci. Technol.* **2016**, *50* (18), 9990−9997.

(28) Appiani, E.; Ossola, R.; Latch, D. E.; Erickson, P. R.; McNeill, K. Aqueous Singlet Oxygen Reaction Kinetics of Furfuryl Alcohol: Effect of Temperature, pH, and Salt Content. *Environ. Sci. Process. Impacts* **2017**, *19* (4), 507−516.

(29) Cook, R. D.; Lin, Y.-H.; Peng, Z.; Boone, E.; Chu, R. K.; Dukett, J. E.; Gunsch, M. J.; Zhang, W.; Tolic, N.; Laskin, A.; et al. Biogenic, Urban, and Wildfire Influences on the Molecular Composition of Dissolved Organic Compounds in Cloud Water. *Atmos. Chem. Phys.* **2017**, *17* (24), 15167−15180.

(30) Buxton, G. V.; Greenstock, C. L.; Helman, W. P.; Ross, A. B. Critical Review of Rate Constants for Reactions of Hydrated

DOI: 10.1021/acs.est.9b01609
Environ. Sci. Technol. 2019, 53, 8553−8562

Electrons, Hydrogen Atoms and Hydroxyl Radicals (·OH/·O $^-$ in Aqueous Solution. *J. Phys. Chem. Ref. Data* **1988**, *17* (2), 513−886.
(31) Davis, C. A.; McNeill, K.; Janssen, E. M.-L. Non-Singlet Oxygen Kinetic Solvent Isotope Effects in Aquatic Photochemistry. *Environ. Sci. Technol.* **2018**, *52* (17), 9908−9916.
(32) Schmidt, R.; Tanielian, C.; Dunsbach, R.; Wolff, C. Phenalenone, a Universal Reference Compound for the Determination of Quantum Yields of Singlet Oxygen $O_2(^1\Delta_g)$ Sensitization. *J. Photochem. Photobiol., A* **1994**, *79* (1), 11−17.
(33) Page, S. E.; Arnold, W. A.; McNeill, K. Terephthalate as a Probe for Photochemically Generated Hydroxyl Radical. *J. Environ. Monit.* **2010**, *12* (9), 1658.
(34) Zhou, X.; Mopper, K. Determination of Photochemically Produced Hydroxyl Radicals in Seawater and Freshwater. *Mar. Chem.* **1990**, *30*, 71−88.
(35) Towne, V.; Will, M.; Oswald, B.; Zhao, Q. Complexities in Horseradish Peroxidase-Catalyzed Oxidation of Dihydroxyphenoxazine Derivatives: Appropriate Ranges for pH Values and Hydrogen Peroxide Concentrations in Quantitative Analysis. *Anal. Biochem.* **2004**, *334* (2), 290−296.
(36) Zhao, B.; Summers, F. A.; Mason, R. P. Photooxidation of Amplex Red to Resorufin: Implications of Exposing the Amplex Red Assay to Light. *Free Radical Biol. Med.* **2012**, *53* (5), 1080−1087.
(37) Sharpless, C. M. Lifetimes of Triplet Dissolved Natural Organic Matter (DOM) and the Effect of $NaBH_4$ Reduction on Singlet Oxygen Quantum Yields: Implications for DOM Photophysics. *Environ. Sci. Technol.* **2012**, *46* (8), 4466−4473.
(38) Haag, W. R.; Hoigne, Juerg Singlet Oxygen in Surface Waters. 3. Photochemical Formation and Steady-State Concentrations in Various Types of Waters. *Environ. Sci. Technol.* **1986**, *20* (4), 341−348.
(39) Marchisio, A.; Minella, M.; Maurino, V.; Minero, C.; Vione, D. Photogeneration of Reactive Transient Species upon Irradiation of Natural Water Samples: Formation Quantum Yields in Different Spectral Intervals, and Implications for the Photochemistry of Surface Waters. *Water Res.* **2015**, *73*, 145−156.
(40) Zepp, R. G.; Schlotzhauer, P. F.; Sink, R. Merritt. Photosensitized Transformations Involving Electronic Energy Transfer in Natural Waters: Role of Humic Substances. *Environ. Sci. Technol.* **1985**, *19* (1), 74−81.
(41) Maizel, A. C.; Remucal, C. K. Molecular Composition and Photochemical Reactivity of Size-Fractionated Dissolved Organic Matter. *Environ. Sci. Technol.* **2017**, *51* (4), 2113−2123.
(42) Lin, P.; Liu, J.; Shilling, J. E.; Kathmann, S. M.; Laskin, J.; Laskin, A. Molecular Characterization of Brown Carbon (BrC) Chromophores in Secondary Organic Aerosol Generated from Photo-Oxidation of Toluene. *Phys. Chem. Chem. Phys.* **2015**, *17* (36), 23312−23325.
(43) Jiang, H.; Jang, M.; Sabo-Attwood, T.; Robinson, S. E. Oxidative Potential of Secondary Organic Aerosols Produced from Photooxidation of Different Hydrocarbons Using Outdoor Chamber under Ambient Sunlight. *Atmos. Environ.* **2016**, *131*, 382−389.
(44) Arakaki, T.; Anastasio, C.; Kuroki, Y.; Nakajima, H.; Okada, K.; Kotani, Y.; Handa, D.; Azechi, S.; Kimura, T.; Tsuhako, A.; et al. A General Scavenging Rate Constant for Reaction of Hydroxyl Radical with Organic Carbon in Atmospheric Waters. *Environ. Sci. Technol.* **2013**, *47* (15), 8196−8203.
(45) Foote, C. S.; Clennan, E. L. Properties and Reactions of Singlet Dioxygen. In *Active Oxygen in Chemistry*; Foote, C. S., Valentine, J. S., Greenberg, A., Liebman, J. F., Eds.; Structure Energetics and Reactivity in Chemistry Series (SEARCH Series); Springer Netherlands: Dordrecht, 1995; pp 105−140.
(46) Aiona, P. K.; Luek, J. L.; Timko, S. A.; Powers, L. C.; Gonsior, M.; Nizkorodov, S. A. Effect of Photolysis on Absorption and Fluorescence Spectra of Light-Absorbing Secondary Organic Aerosols. *ACS Earth Space Chem.* **2018**, *2* (3), 235−245.
(47) Kautzman, K. E.; Surratt, J. D.; Chan, M. N.; Chan, A. W. H.; Hersey, S. P.; Chhabra, P. S.; Dalleska, N. F.; Wennberg, P. O.; Flagan, R. C.; Seinfeld, J. H. Chemical Composition of Gas- and Aerosol-Phase Products from the Photooxidation of Naphthalene. *J. Phys. Chem. A* **2010**, *114* (2), 913−934.
(48) Ji, Y.; Zhao, J.; Terazono, H.; Misawa, K.; Levitt, N. P.; Li, Y.; Lin, Y.; Peng, J.; Wang, Y.; Duan, L.; et al. Reassessing the Atmospheric Oxidation Mechanism of Toluene. *Proc. Natl. Acad. Sci. U. S. A.* **2017**, *114* (31), 8169−8174.
(49) Yassine, M. M.; Harir, M.; Dabek-Zlotorzynska, E.; Schmitt-Kopplin, P. Structural Characterization of Organic Aerosol Using Fourier Transform Ion Cyclotron Resonance Mass Spectrometry: Aromaticity Equivalent Approach: Characterization of Organic Aerosol Using FTICRMS. *Rapid Commun. Mass Spectrom.* **2014**, *28* (22), 2445−2454.
(50) Weishaar, J. L.; Aiken, G. R.; Bergamaschi, B. A.; Fram, M. S.; Fujii, R.; Mopper, K. Evaluation of Specific Ultraviolet Absorbance as an Indicator of the Chemical Composition and Reactivity of Dissolved Organic Carbon. *Environ. Sci. Technol.* **2003**, *37* (20), 4702−4708.
(51) Haynes, J. P.; Miller, K. E.; Majestic, B. J. Investigation into Photoinduced Auto-Oxidation of Polycyclic Aromatic Hydrocarbons Resulting in Brown Carbon Production. *Environ. Sci. Technol.* **2019**, *53* (2), 682−691.
(52) Rosado-Lausell, S. L.; Wang, H.; Gutiérrez, L.; Romero-Maraccini, O. C.; Niu, X.-Z.; Gin, K. Y. H.; Croué, J.-P.; Nguyen, T. H. Roles of Singlet Oxygen and Triplet Excited State of Dissolved Organic Matter Formed by Different Organic Matters in Bacteriophage MS2 Inactivation. *Water Res.* **2013**, *47* (14), 4869−4879.
(53) McWhinney, R. D.; Zhou, S.; Abbatt, J. P. D. Naphthalene SOA: Redox Activity and Naphthoquinone Gas−Particle Partitioning. *Atmos. Chem. Phys.* **2013**, *13* (19), 9731−9744.
(54) Escalada, J. P.; Pajares, A.; Gianotti, J.; Massad, W. A.; Bertolotti, S.; Amat-Guerri, F.; García, N. A. Dye-Sensitized Photodegradation of the Fungicide Carbendazim and Related Benzimidazoles. *Chemosphere* **2006**, *65* (2), 237−244.
(55) Abdelraheem, W. H. M.; He, X.; Komy, Z. R.; Ismail, N. M.; Dionysiou, D. D. Revealing the Mechanism, Pathways and Kinetics of UV 254nm/H_2O_2-Based Degradation of Model Active Sunscreen Ingredient PBSA. *Chem. Eng. J.* **2016**, *288*, 824−833.
(56) Kraljić, I.; Sharpatyi, V. A. Determination of Singlet Oxygen Rate Constants in Aqueous Solutions. *Photochem. Photobiol.* **1978**, *28* (4−5), 583−586.
(57) Ching, T.-L.; Haenen, G. R. M. M.; Bast, A. Cimetidine and Other H_2 Receptor Antagonists as Powerful Hydroxyl Radical Scavengers. *Chem.-Biol. Interact.* **1993**, *86* (2), 119−127.
(58) Mercader, A. G.; Duchowicz, P. R.; Fernández, F. M.; Castro, E. A.; Cabrerizo, F. M.; Thomas, A. H. Predictive Modeling of the Total Deactivation Rate Constant of Singlet Oxygen by Heterocyclic Compounds. *J. Mol. Graphics Modell.* **2009**, *28* (1), 12−19.
(59) Iddon, B.; Phillips, G. O.; Robbins, K. E.; Davies, J. V. Radiation Chemistry of Aqueous Solutions of Indole and Its Derivatives. *J. Chem. Soc. B* **1971**, *6*, 1887−1892.
(60) Kawanishi, S.; Sakurai, H. Differential Anti-Lipid Peroxidative Activity of Melatonin. *Naturwissenschaften* **2002**, *89* (1), 31−33.
(61) Li, Y. J.; Huang, D. D.; Cheung, H. Y.; Lee, A. K. Y.; Chan, C. K. Aqueous-Phase Photochemical Oxidation and Direct Photolysis of Vanillin − a Model Compound of Methoxy Phenols from Biomass Burning. *Atmos. Chem. Phys.* **2014**, *14* (6), 2871−2885.
(62) Machado, A. E. H.; Gomes, A. J.; Campos, C. M. F.; Terrones, M. G. H.; Perez, D. S.; Ruggiero, R.; Castellan, A. Photoreactivity of Lignin Model Compounds in the Photobleaching of Chemical Pulps 2. Study of the Degradation of 4-Hydroxy-3-Methoxy-Benzaldehyde and Two Lignin Fragments Induced by Singlet Oxygen. *J. Photochem. Photobiol., A* **1997**, *110* (1), 99−106.
(63) Tratnyek, P. G.; Hoigne, J. Oxidation of Substituted Phenols in the Environment: A QSAR Analysis of Rate Constants for Reaction with Singlet Oxygen. *Environ. Sci. Technol.* **1991**, *25* (9), 1596−1604.
(64) Lauraguais, A.; Coeur-Tourneur, C.; Cassez, A.; Seydi, A. Rate Constant and Secondary Organic Aerosol Yields for the Gas-Phase Reaction of Hydroxyl Radicals with Syringol (2,6-Dimethoxyphenol). *Atmos. Environ.* **2012**, *55*, 43−48.

DOI: 10.1021/acs.est.9b01609
Environ. Sci. Technol. 2019, 53, 8553−8562

(65) Scully, F. E.; Hoigné, J. Rate Constants for Reactions of Singlet Oxygen with Phenols and Other Compounds in Water. *Chemosphere* **1987**, *16* (4), 681−694.
(66) Biswal, J.; Paul, J.; Naik, D. B.; Sarkar, S. K.; Sabharwal, S. Radiolytic Degradation of 4-Nitrophenol in Aqueous Solutions: Pulse and Steady State Radiolysis Study. *Radiat. Phys. Chem.* **2013**, *85*, 161−166.
(67) Lundeen, R. A.; Janssen, E. M.-L.; Chu, C.; Mcneill, K. Environmental Photochemistry of Amino Acids, Peptides and Proteins. *Chimia* **2014**, *68* (11), 812−817.
(68) Mártire, D. O.; Braslavsky, S. E.; García, N. A. Sensitized Photo-Oxidation of Dihydroxybenzenes and Chlorinated Derivatives. A Kinetic Study. *J. Photochem. Photobiol., A* **1991**, *61* (1), 113−124.
(69) Smith, J. D.; Kinney, H.; Anastasio, C. Phenolic Carbonyls Undergo Rapid Aqueous Photodegradation to Form Low-Volatility, Light-Absorbing Products. *Atmos. Environ.* **2016**, *126*, 36−44.
(70) McConville, M. B.; Mezyk, S. P.; Remucal, C. K. Indirect Photodegradation of the Lampricides TFM and Niclosamide. *Environ. Sci. Process. Impacts* **2017**, *19* (8), 1028−1039.
(71) Mashayekhy Rad, F.; Zurita, J.; Gilles, P.; Rutgeerts, L. A. J.; Nilsson, U.; Ilag, L. L.; Leck, C. Measurements of Atmospheric Proteinaceous Aerosol in the Arctic Using a Selective UHPLC/ESI-MS/MS Strategy. *J. Am. Soc. Mass Spectrom.* **2019**, *30* (1), 161−173.
(72) Teich, M.; van Pinxteren, D.; Wang, M.; Kecorius, S.; Wang, Z.; Muller, T.; Mocnik, G.; Herrmann, H. Contributions of Nitrated Aromatic Compounds to the Light Absorption of Water-Soluble and Particulate Brown Carbon in Different Atmospheric Environments in Germany and China. *Atmos. Chem. Phys.* **2017**, *17* (3), 1653−1672.
(73) Wang, Y.; Hu, M.; Wang, Y.; Zheng, J.; Shang, D.; Yang, Y.; Liu, Y.; Li, X.; Tang, R.; Zhu, W.; Du, Z.; Wu, Y.; Guo, S.; Wu, Z.; Lou, S.; Hallquist, M.; Yu, J. Z. The Formation of Nitro-Aromatic Compounds under High NO_x and Anthropogenic VOC Conditions in Urban Beijing, China. *Atmos. Chem. Phys.* **2019**, *19* (11), 7649−7665.
(74) Li, Y. J.; Huang, D. D.; Cheung, H. Y.; Lee, A. K. Y.; Chan, C. K. Aqueous-Phase Photochemical Oxidation and Direct Photolysis of Vanillin − a Model Compound of Methoxy Phenols from Biomass Burning. *Atmos. Chem. Phys.* **2014**, *14* (6), 2871−2885.
(75) Vione, D.; Albinet, A.; Barsotti, F.; Mekic, M.; Jiang, B.; Minero, C.; Brigante, M.; Gligorovski, S. Formation of Substances with Humic-like Fluorescence Properties, upon Photoinduced Oligomerization of Typical Phenolic Compounds Emitted by Biomass Burning. *Atmos. Environ.* **2019**, *206*, 197−207.
(76) Cory, R. M.; McNeill, K.; Cotner, J. P.; Amado, A.; Purcell, J. M.; Marshall, A. G. Singlet Oxygen in the Coupled Photochemical and Biochemical Oxidation of Dissolved Organic Matter. *Environ. Sci. Technol.* **2010**, *44* (10), 3683−3689.
(77) Badali, K. M.; Zhou, S.; Aljawhary, D.; Antiñolo, M.; Chen, W. J.; Lok, A.; Mungall, E.; Wong, J. P. S.; Zhao, R.; Abbatt, J. P. D. Formation of Hydroxyl Radicals from Photolysis of Secondary Organic Aerosol Material. *Atmos. Chem. Phys.* **2015**, *15* (14), 7831−7840.

DOI: 10.1021/acs.est.9b01609
Environ. Sci. Technol. 2019, 53, 8553−8562